Phosphor coated NiO-based planar inverted organometallic halide perovskite solar cells with enhanced efficiency and stability

Jin Cui,[1⊥] Pengfei Li,[2⊥] Zhifan Chen, [1⊥] Kun Cao,[1] Dan Li,[1] Junbo Han,[3] Yan Shen,[1] Mingying Peng,[2,*] Yong Qing Fu[4] and Mingkui Wang[1,*]

[1] *Wuhan National Laboratory for Optoelectronics, School of Optical and Electronic Information, Huazhong University of Science and Technology, Wuhan, Hubei 430074, P. R. China*

[2] *The China-Germany Research Center for Photonic Materials and Device, The State Key Laboratory of Luminescent Materials and Devices, School of Materials Science and Engineering, South China University of Technology, Guangzhou 510640, P. R. China*

[3] *Wuhan National High Magnetic Field Center, Huazhong University of Science and Technology, 1037 Luoyu Road, Wuhan 430074, Hubei, P. R. China*

[4] *Department of Physics and Electrical Engineering, Faculty of Engineering and Environment, Northumbria University, Newcastle Upon Tyne, NE1 8ST, UK*

[⊥] *Contributed equally.*

This work investigates non-rare-earth phosphor ($Sr_4Al_{14}O_{25}:Mn^{4+}$, 0.5%Mg) with intensively red luminescence as a luminescent down-shifting layer for perovskite solar cells. The power conversion efficiency of the fabricated device with a structure of NiO/$CH_3NH_3PbI_3$/[6,6]-phenyl C_{61}-butyric acid methyl ester/Au coated with phosphor layer shows a 10% increase as compared with that of the control devices. Importantly, the phosphor layer coating can realize UV-protection as well as waterproof capability, achieving a reduced moisture-degradation of $CH_3NH_3PbI_3$ perovskite upon applying an UV irradiation. Therefore, perovskite devices using this luminescent coating show a combined enhancement in both UV down-shifting conversion and long term stability. This can be expanded as a promising encapsulation technique in the perovskite solar cell community.

A significant progress has been achieved over the past few years for the development of solar cells using hybrid lead halide perovskite as next generation light harvester.[1-4] Currently, the certified power conversion efficiency (PCE) for the perovskite solar cells is dramatically increased over 22.1% for the lab-scale devices.[5] In addition to the high PCE, the perovskite solar cells take advantages of low cost and solution processability, making them as a promising photovoltaic technology till date.[6,7] At present, excellent solar cell performance has been achieved for devices based on inorganic-organic hybrid lead perovskites. However, a number of obstacles limit its commercialization, including long-term device stability in operation conditions with oxygen, humidity/rain/ice, heat, and ultra-violet (UV) light exposure. Previous works have pointed

* corresponding author: mingkui.wang@hust.edu.cn; pengmingying@scut.edu.cn

This manuscript was accepted by Appl. Phys. Lett. Click here to see the version of record.

out that perovskite solar cells with particular device structures can be stable when devices are kept in dark and dry air atmosphere at room temperature.[8-11] The instability of devices in operation conditions mainly comes from the degradation of perovskite materials.[12-14] Moisture, UV light, and temperature are susceptible to cause degradation of organic-inorganic perovskite. Kelly *et al*. reported a quantitative and systematic investigation of perovskite degradation processes by using in situ absorption spectroscopy and in situ grazing incidence X-ray diffraction (XRD) to monitor phase changes in a controlled relative humidity of an environmental chamber.[15] They demonstrated the formation of a hydrated intermediate containing isolated $PbI_6^{(4-)}$ octahedra as the first step of the degradation mechanism. Therefore, it is highly desirable to find suitable strategies to develop stable perovskite devices for future application, which should be inert moisture-sensitive, especially when elevated temperature and/or electrical bias are applied.[15-18] Material engineering has been considering as one of the promising strategies to enhance the stability of inorganic/organic halide lead perovskites. Iodide-chloride mixed halide perovskite $MAPbI_xCl_{3-x}$ was reported to be more stable than single-halide perovskite $MAPbI_3$ in ambient atmosphere.[19] The stability of $MAPbI_3$ in humid air could be significantly improved by doping with bromide.[20] Tuning the tolerance factor is also an effective way to stabilize perovskite structure for solar cell applications. Extensive researches have been done on formanidinium methylammounium lead iodide ($FAPbI_3$) due to its broad light absorption and good thermal stability.[21,22] Despite of the significant improvements have been evidenced by carefully controlling of components in perovskite solar cells,[24-26] the stability of organic-inorganic hybrid lead perovskite solar cell devices is still unsatisfactory, particularly their outdoor stability and long term performance in the presence of moisture and light illumination. For example, most of investigation have found this degradation process could be easily accelerated by UV light exposure in TiO_2-based perovskite solar cells.[23] The UV-degradation in these cells were generally suffered from a deep trapping of injected electrons within newly available sites in the TiO_2 nanocrystal semiconductor. This instability of perovskite solar cells under an UV exposure can be rectified by removing TiO_2 scaffold.

Likewise, coating the photovoltaic devices with antireflection and self-cleaning function layers has been designed for silicon and polymer solar cells to increase their power conversion efficiency as well as ultraviolet light stability.[27-29] Griffini *et al*. reported on the conversion and manipulation of light *via* luminescent down-shifting (LDS) by an elegant combination of lanthanide-doped polymer-derived ceramics incorporated with versatile nanopatterns for advanced optoelectronics, showing distinctively enhanced PCE and lifetime mainly attributed to the nanopattern assisted strong LDS property.[30] Chander *et al*. reported a transparent LDS $YVO_4:Eu^{3+}$ nano-phosphor layer to mitigate UV degradation in the TiO_2-based perovskite solar cells, showing an improvement in stability under prolonged illumination and photocurrent due to LDS of incident UV photons into additional red photons.[31] Therefore, it's worth to address the importance of UV protection with

This manuscript was accepted by Appl. Phys. Lett. Click here to see the version of record.

functional coating for the inverted planar perovskite solar cells without using TiO_2. Herein, we investigated a multifunctional coating for the NiO-based inverted perovskite solar cell devices, which incorporates an combined ability of LDS and UV-screening as well as waterproof. This coating layer uses a non-rare-earth phosphor ($Sr_4Al_{14}O_{25}:Mn^{4+}$, 0.5% Mg, SAM, hereafter) particles embedded in PMMA (polymethylmethacrylate). Such a phosphor exhibits higher intense red luminescence than that of the commercial Mn^{4+} phosphors due to the inclusion of Mg^{2+}.[32] Fig. 1a depicts the device architecture for the NiO-based $CH_3NH_3PbI_3$ solar cell with coating on the top of FTO glass and the corresponding molecular structure of SAM. The $MAPbI_3$ films were directly deposited onto the substrates pre-coated with the NiO using a one-step spin-coating method. Fig. 1b shows the absorption (left ordinate) and emission spectra (right ordinate) of SAM/PMMA films at room temperature. A broad excitation band appears in the range from 290-520 nm, which implies that this phosphor is suitable to be excited with an UV light. As a proof of concept, when the SAM/PMMA film is excited with UV-light (λ=320 nm), a strong red emission peak between 625 and 670 nm with a sharp peak at about 650 nm can be observed in the emission spectrum of the phosphor (Fig. 1b). This is attributed to the typical emission of Mn^{4+}.[32,33] The internal quantum efficiency was measured to be 38 and 35% for the excitation wavelengths of 380 and 470 nm, respectively, for the SAM film.[32] The inset of Fig. 1b shows an optical image of a phosphor film (on quartz) illuminated by UV light at λ~360 nm, exhibiting a uniform red emission over the entire area. In brief, the SAM/PMMA LDS film can efficiently convert ultraviolet light to visible light. We expect this certainly develops functionality for harvesting ultraviolet light and thus reduces a direct absorption of the $CH_3NH_3PbI_3$ active layer in the ultraviolet region. Fig. 1c compares the optical transparency for the FTO glass deposited with SAM/PMMA films, showing that the transmission decreases as the amount of SAM increases in the film. In this work the FTO glass coated with a 1.2 mg mL^{-1} SAM/PMMA layer was selected for further experiments.

To reveal the impact from UV-light on degradation, we first compared the $CH_3NH_3PbI_3$ films coated with/without (W/O) SAM/PMMA exposure to irradiation in different atmospheres (see the scheme in Fig. 2a). The fresh prepared bare $CH_3NH_3PbI_3$ perovskite films were deposited upon FTO glass substrates. During the test, sample A was completely kept in dark. Sample C was coated with SAM/PMMA onto the FTO glass and exposed to light illumination. For comparison, sample B was directly exposed to the UV-light *via* the $CH_3NH_3PbI_3$ film. Fig. S1 (in the supplementary information) shows images of the experimental instruments. The measurements were performed under UV light (λ~360 nm, 12 W) or yellow light (λ~575-595 nm) for 15 hours in ambient air (30-50% relative humidity, RH) or dry air (H_2O<0.1 ppm), respectively.

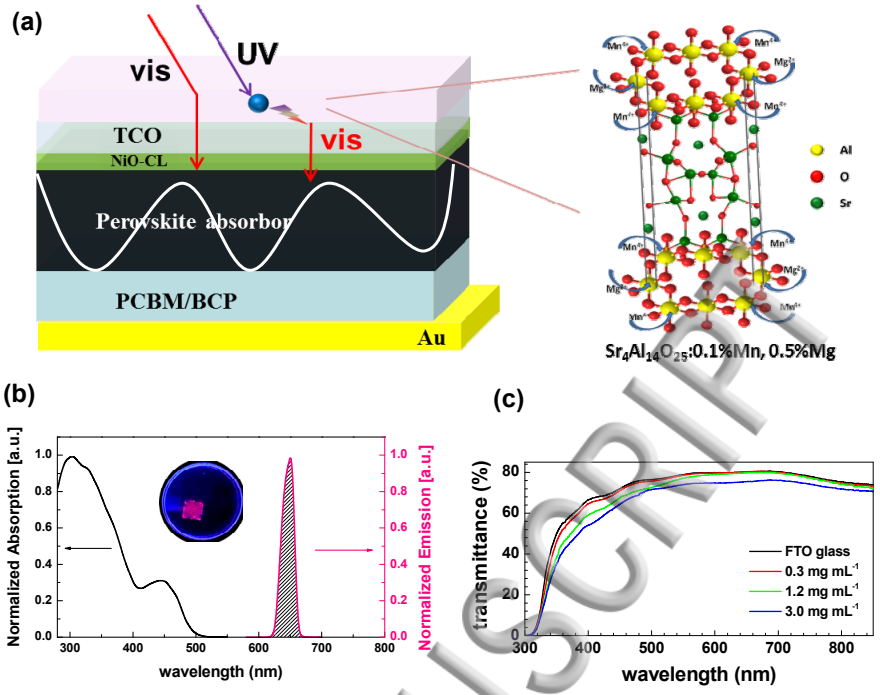

FIG. 1 a) Schematic of perovskite solar cell structure with SAM/PMMA down-shifting layer coated on the FTO glass surface. b) Absorption (left ordinate) and emission (right ordinate) spectra of SAM/PMMA film. Absorbed UV light is down-shifted to the red light region (around 650 nm). Insert shows a photograph of a 1.2 mg mL^{-1} doped SAM/PMMA layer coated glass substrate recorded under ultraviolet (λ~360 nm) illumination. c) Transmission of FTO glasses coated by SAM/PMMA layer with varying SAM phosphor concentration.

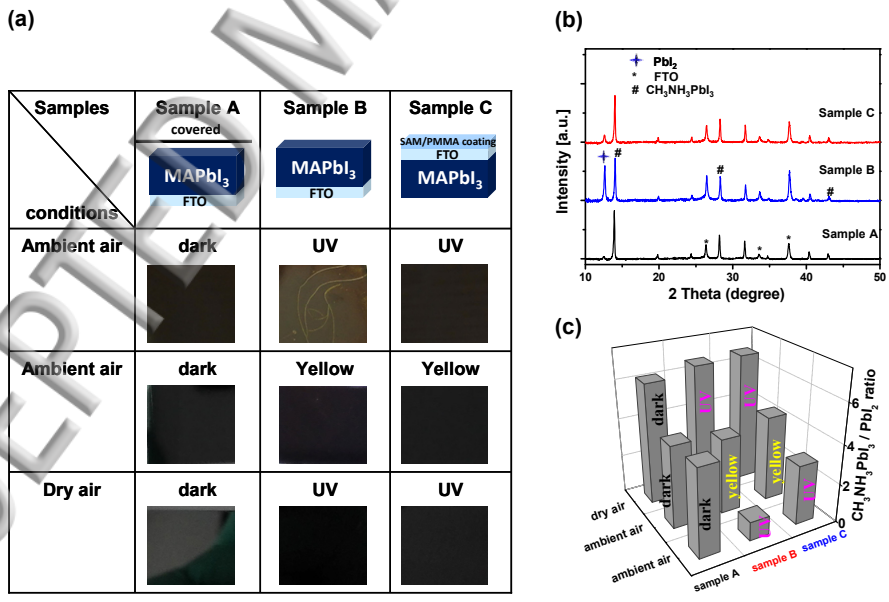

FIG. 2 a) The schematic for the degradation monitoring and optical images of $CH_3NH_3PbI_3$ films after test in different atmosphere; b) XRD patterns of $CH_3NH_3PbI_3$ films of different samples under ambient air condition with UV irradiation for 15 hours; c) the $CH_3NH_3PbI_3/PbI_2$ ratio calculated from the integrated intensities of $CH_3NH_3PbI_3$ and PbI_2 peaks appearing in XRD patterns for different samples.

This manuscript was accepted by Appl. Phys. Lett. Click here to see the version of record.

Fig. 2a also shows the optical images of films after irradiation test. We observed that, when testing in ambient air with UV-irradiation, sample B showed mostly obvious color change. This result was further testified with UV-visible absorption spectroscopy measurements as presented in Fig. S2. Compare to films tested in dark (for sample A) or covered by SAM/PMMA coating (for sample C), the sample B with perovskite exposed to UV-light showed very much decreased light absorption after the irradiation test. PbI_2 are mostly suggested as the product for the degradation of $CH_3NH_3PbI_3$ film in this case.[15-18] In order to qualify the extent of degradation for the perovskite films, we calculated the ratio of $CH_3NH_3PbI_3/PbI_2$ to inform the effect from different atmosphere onto the degradation by integration the intensity of peaks appearing around 14.1 and 12.7 in the XRD patterns collected from each sample after test (Fig. 2b). The peaks at 2θ angles of 14.1° along with 28.4° and 43.1° correspond to the tetragonal phase of $CH_3NH_3PbI_3$, while the peak at around 2θ=12.7 corresponds to the pure crystal PbI_2.[34] A higher $CH_3NH_3PbI_3/PbI_2$ ratio indicates slower $CH_3NH_3PbI_3$ degradation. In this study, it was found that the ratio of $CH_3NH_3PbI_3/PbI_2$ for sample A (totally in dark) decreased from about 6 in the case of dry air to ~4 in the case of ambient air. This result indicates $CH_3NH_3PbI_3$ easily degrades into PbI_2 in the presence of H_2O even the sample is stored in dark. Furthermore, when the measurement was performed under exposure to UV-irradiation in dry air condition, the samples B and C unexpectedly remained their color. This implies the tolerance of $CH_3NH_3PbI_3$ to the UV-irradiation if the atmosphere is free of moisture. The negligible color change was further confirmed with XRD results (see Fig. S3a). As shown in Fig. 2c, the samples B measured in dry air kept a higher $CH_3NH_3PbI_3/PbI_2$ ratio (~6) than that in ambient air (<1) when exposed to UV-light. This result indicates that PbI_2 content dramatically increases in presence of moisture and UV irradiation. Correspondingly, the color of sample B turned from black into yellow within 15 hours (Fig. 2a). We conclude that the UV irradiation accelerates the degradation of $CH_3NH_3PbI_3$ material in the presence of moisture. This degradation can be largely reduced if a SAM/PMMA coating (sample C) was used onto the FTO side through which the irradiation gets into the perovskite layer. The $CH_3NH_3PbI_3/PbI_2$ ratio was estimated to be ~3 for sample C stored in ambient air in combination with UV expose. This result demonstrates that the SAM/PMMA coating could effectively retard the degradation of $CH_3NH_3PbI_3$. This would benefit perovskite devices as discussed below.

Recently, Barnes *et al*. reported on degradation of perovskite with ellipsometry and XRD characterization and found the primary formation of a monohydrate phase for $CH_3NH_3PbI_3$ in the presence of moisture.[35] This product was observed in equilibrium with a small amount of the dehydrate phase, depending on the time and intensity of moisture exposure.[35] Evaporation of HI along with elevated temperatures accelerated this process as well.[17] Since PbI_2 can be found in the perovskite film after UV exposure in the presence of moisture, we propose that the monohydrate $CH_3NH_3PbI_3 \cdot H_2O$ phase with loose bound characterization in the $CH_3NH_3PbI_3$ films degrades with increasing incident high-energy photons and

This manuscript was accepted by Appl. Phys. Lett. Click here to see the version of record.

eventually decomposes to PbI_2. Fig. 3 schemes the $CH_3NH_3PbI_3$ degradation process in the presence of moisture accelerated by UV light. We suggest that the presence of a long-term UV irradiation can greatly accelerate this process and thus shorten the degradation into several hours. To test this hypothesis, the samples B and C were irradiated with yellow light (λ~575-595 nm) in ambient air (30-50% RH), and their XRD results and corresponding $CH_3NH_3PbI_3/PbI_2$ ratio are presented in Figs. 2c and S3. Both samples are much stable in ambient air under yellow irradiation compared to UV irradiation.

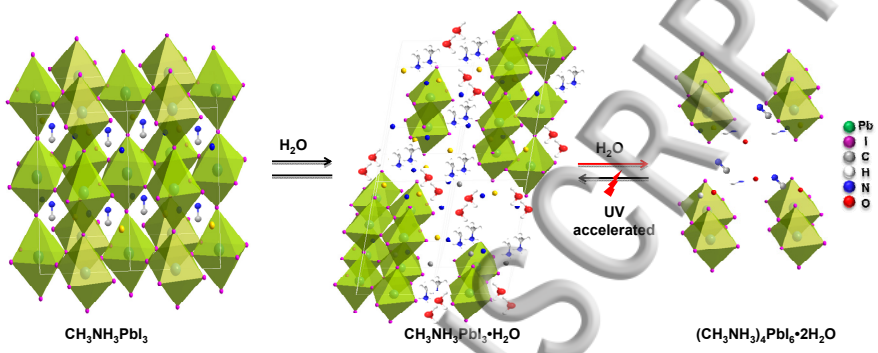

FIG. 3 Schematic of the $CH_3NH_3PbI_3$ degradation process in the presence of moisture accelerated by UV light.

Photovoltaic characterization was performed with different amount of phosphor to estimate the possibility of enhancing light harvesting efficiency for the perovskite devices. Fig. 4a compare the photocurrent-voltage curves for the devices with and without coating. The photovoltaic parameters are J_{SC}~19.6 mA cm^{-2}, V_{OC} ~ 1.04V, FF ~0.7, yielding a PCE ~14% for the perovskite solar cell with a SAM coating at a concentration of 1.2 mg mL^{-1}. Under the same condition, the J_{SC} of device without coating is about 18.2 mA cm^{-2} with a PCE of 12.6%. Therefore, there is a significant ~7.7% increase in the short circuit current density if the phosphor coating is used. This was confirmed by scratch coating off the FTO glass, the J_{SC} decreased to that of the bare device as shown in Fig. 4a. As shown in the inset, the devices with SAM/PMMA coating at a concentration of 0.3 mg mL^{-1} or 1.2 mg mL^{-1} showed higher photocurrents comparing to the control devices without coating. However, it was found a reduction of values of J_{SC} for the device using coating containing higher concentration of SAM (>3 mg mL^{-1}) due to an unbalanced transparency loss (the inset of Fig. 4a). Fig. 4b shows the IPCE curves (left ordinate) for devices with and without coating. Both of them exhibited similar spectral responses in the wavelength range from 500 to 800 nm. However, it is noted that the device with coating (1.2 mg mL^{-1}) showed higher IPCE response in the shorter wavelength region. The Δ_{IPCE} spectrum in Fig. 4b (right ordinate) was obtained by taking the difference in the IPCE spectra between the two devices. A broad band was observed in the wavelength region of 350-500 nm. This result agrees well with the measured absorption region of SAM material (Fig. 1b). The integrated current density of the enhanced IPCE value is calculated to be 1.29 mA cm^{-2} (right ordinate), which can be contributed to the photocurrent enhancement. We expect that the J_{SC} values

could be further increased by using phosphor of a size below 10 nm in terms of reduction of long wavelength scattering effect and transparency loss. The IPCE response depends on the efficiencies of charge injection, light harvesting ability and charge collection.[36] Considering the high absorbance of $CH_3NH_3PbI_3$ perovskite film (>2 in a wide wavelength range) and high photocurrent density of most reported devices (~20 mA cm^{-2}), the latter two efficiencies are assumed to be unit for both devices in this study. As shown in Fig. 4b, the IPCE values for the device without coating are less than 60% in the range of 340-500 nm, indicating that the charge injection efficiency is less effective in short wavelength region. This could be correlated to different hot-hole (electron) cooling mechanisms for lead-lodide perovskite excited by photons with different energy. Therefore, we suggest the observed improvement for the device with coating can be due to the LDS effect of the SAM/PMMA, which convert the short wavelength photons into long wavelength photons.

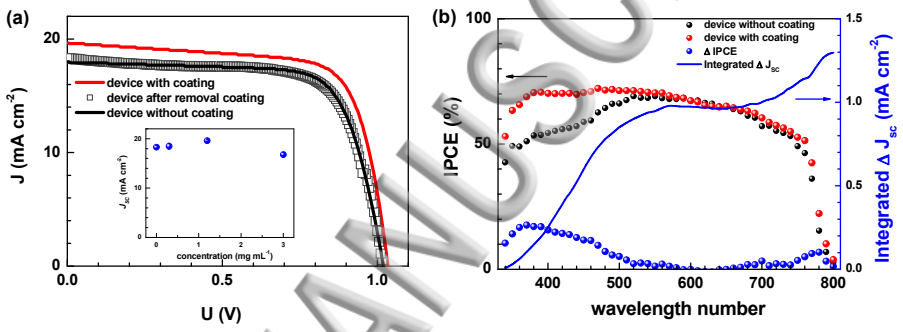

FIG. 4 (a) Current density-voltage plots measured under AM1.5 simulated sunlight of 100 mW cm^{-2} irradiance of the $NiO/CH_3NH_3PbI_3$/PCBM perovskite solar cell devices with and without SAM/PMMA coating at a concentration of 1.2 mg mL^{-1}. The inset shows the photocurrent density variation with SAM concentration in SAM/PMMA coating. (b) IPCE spectrum for the devices with and without coating. The integrated ΔJ is contributed from the IPCE difference.

Fig. 5a shows the variation of PCEs with time for the perovskite solar cell devices with/without the SAM/PMMA LDS coating under a relatively low light intensity of about 25 mW cm^{-2}. A xenon lamp was used as a light source to simulate sunlight containing UV-lights. The low light intensity was selected in this study was due to a fast degradation of $CH_3NH_3PbI_3$ devices under full solar simulator irradiation in ambient air. The temperature was controlled in the range of 25-30 ^oC with a RH value below 30% during the measurement. The devices without SAM/PMMA coating showed dramatically degradation in PCE, which failed to work after 30 hours. The degradation for the control experiment could be due to an adsorption of oxygen/water by the PCBM (the PCBM layer itself can degrade in ambient air through adsorption of oxygen or water), and/or an incomplete coverage of the perovskite film by the PCBM, thus leading to a rapid chemical reaction between the Au electrode and the $CH_3NH_3PbI_3$ when exposure to the ambient environment.[37,38] The devices with SAM/PMMA coating at the FTO glass showed a better stability in terms of PCE. The efficiency of the device retains more than 55% of the initial values. The efficiency of these devices retained more than 55% of the initial values. By contrast, the control device lost completely its performance, mainly on the photocurrent (Fig. S4). It is quite evident that the perovskite devices with SAM/PMMA

coating are indeed considerably resilient to UV irradiation. As discussed above, the enhanced device stability could be contributed to the SAM/PMMA coating, which suppresses the $CH_3NH_3PbI_3$ monohydrate phase degradation stemmed in the presence of moisture and full spectral sunlight irradiation.

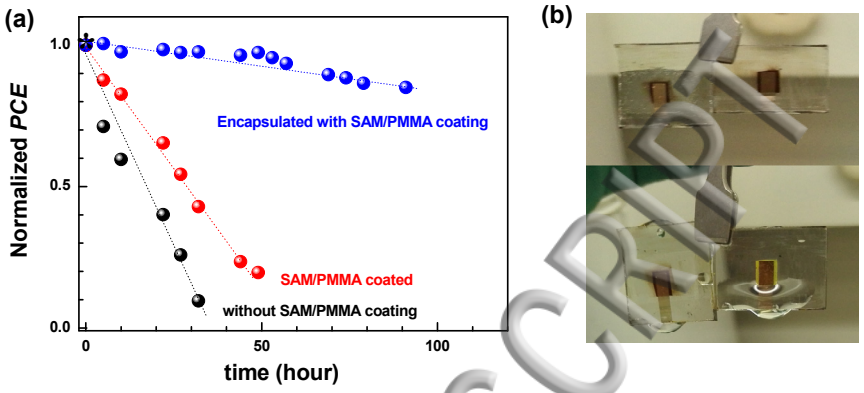

FIG. 5 (a) The performance stability of the cells with and without SAM/PMMA LD coating. The cells were kept in a dry cabinet (< 30% humidity) at 25 mW cm^{-2} illumination provided by a solar simulator and measured in ambient air under AM1.5G. (b) A photograph of a complete perovskite solar cell employing a SAM/PMMA LD coating encapsulation (left) under the water flow, compared with the none coated device (right).

In order to monitor the long-term stability under visible-light soak, the device was encapsulated by a layer of SAM/PMMA on the back counter electrode in dry argon (Ar_2) filled glove box. When exposed to a steady stream of running water, the encapsulated device (left) showed no sign of color change. However, the unsealed device (right) showed dramatic color change from dark black to white (Fig. 5b). Further investigation of stability under illumination revealed that devices with SAM/PMMA encapsulation layers at the front side (FTO glass) and back side (Au electrode) maintained ~80% of its initial values after 90 hours (Fig. 5a). Therefore, the "water-resistant" SAM/PMMA layer offers an enhanced protection of the solar cell, being served as an easy-cleaning protective coating.

In summary, we have elucidated that in ambient air, applying UV irradiation rapidly accelerates the degradation of the perovskite material, leading to broking the reversible equilibrium of $CH_3NH_3PbI_3$ monohydrate phase with the dehydrate phase, and eventually decomposing to PbI_2. This effect has been largely overlooked, since light LEDs or UV filtered solar simulators are commonly employed. A multi-functional coating was developed in this work incorporating LDS with function of UV-screening and waterproof for utilization in NiO-based planar perovskite solar cell devices. This coating consists of room temperature-curable resin containing a non-rare-earth phosphor complex that acts as down-shifting material to convert UV photons into valuable visible light. The perovskite solar cell devices incorporating this functional coating system were found to show a 10% relative increase in power conversion efficiency as compared with control uncoated devices, mainly from an enhancement in photocurrent. Stability improvement of perovskite solar cells with SAM/PMMA coating were also

systematically demonstrated. The general approach presented in this study to simultaneously improve performance and stability of perovskite solar cell devices could be readily extended to a large variety of cost effective nano-phosphor and transparent perovskite solar cell systems, thus enabling fabrication of highly efficient and stable perovskite solar cell system in an easy and versatile approach.

Supplementary Material:

See supplementary material for the complete characterization experiment, experimental instrument images, XRD characterization results and photocurrent stability data.

Acknowledgement:

Financial support from the National Basic Research Program of China (Grants 2013CB922104 and 2014CB643506), the National Natural Science Foundation of China (Grant No. 51322208), Guangdong Natural Science Foundation for Distinguished Young Scholars (Grant No. S20120011380), the Royal Academy of Engineering-Research Exchange with China and India, the Director Fund of the Wuhan National Laboratory for Optoelectronics, and Wuhan National High Magnetic Field Center (2015KF18) is gratefully acknowledged. We thank the Analytical and Testing Centre at the HUST for performing characterization of various samples.

References:

[1] H. Zhou, Q. Chen, G. Li, S. Luo, T. Song, H. Duan, Z. Hong, J. You, Y. Liu and Y. Yang, Science 345, 542 (2014).

[2] O. Malinkiewicz, A. Yella, Y. Lee, G. Espallargas, M. Graetzel, M. Nazeeruddin and H. Bolink, Nat. Photonics 8, 128 (2014).

[3] Y. Yuan, J. Li and M. Wang, Acta Phys. Sin. 64, 038405 (2015).

[4] J. Cui, H. Yuan, J. Li, X. Xu, Y. Shen, H. Lin and M. Wang, Sci. Tech. Adv. Mat. 16, 036004 (2015).

[5] W. Yang, J. Noh, N. Jeon, Y. Kim, S. Ryu, J. Seo and S. Seok, Science 348, 1234 (2015).

[6] J. Gong, S. Darling and F. You, Energy Environ. Sci. 8, 1953 (2015).

[7] N. Espinosa, L. Serrano-Luján, A. Ur bina and F. Krebs, Sol. Energy Mater. Sol. Cells 137, 303 (2015).

[8] H. Kim, C. Lee, J. Im, K. Lee, T. Moehl, A. Marchioro, S. Moon, R. Humphry-Baker, J. Yum, J. Moser, M. Grätzel and N. Park, Sci. Rep. 2, 591 (2012).

[9] G. Niu, W. Li, F. Meng, L. Wang, H. Dong and Y. Qiu, J. Mater. Chem. A 2, 705 (2014).

[10] K. Cao, J. Cui, H. Zhang, H. Li, J. Song, Y. Shen, Y. Cheng and M. Wang, J. Mater. Chem. A 3, 9116 (2015).

[11] K. Cao, Z. Zuo, J. Cui, Y. Shen, T. Moehl, S. Zakeeruddin, M. Grätzel and M. Wang, Nano Energy 17, 171 (2015).

[12] K. Cao, H. Li, S. Liu, J. Cui, Y. Shen, M. Wang, Nanoscale, 8, 8839 (2016).

[13] S. Ito, S. Tanaka, K. Manabe and H. Nishino, J. Phys. Chem. C 118, 16995 (2014).

[14] W. Li, H. Dong, L. Wang, N. Li, X. Guo, J. Li and Y. Qiu, J. Mater. Chem. A 2, 13587 (2014).

[15] J. Yang, B. Siempelkamp, D. Liu and T. Kelly, ACS Nano 9, 1955 (2015).

[16] J. Christians, P. Herrera and P. Kamat, J. Am. Chem. Soc. 137, 1530 (2015).

[17] S. Habisreutinger, T. Leijtens, G. Eperon, S. Stranks, R. Nicholas and H. Snaith, Nano Lett. 14, 5561 (2014).

[18] T. Leijtens, E. Hoke, G. Grancini, D. Slotcavage, G. Eperon, J. Ball1, M. Bastiani, A. Bowring, N. Martino, K. Wojciechowski, M. McGehee, H. Snaith, and A. Petrozza, Adv. Energy Mater. 5, 201500962 (2015).

[19] M. Lee, J. Teuscher, T. Miyasaka, T. Murakami and H. Snaith, Science 338, 643 (2012).

[20] J. Noh, S. Im, J. Heo, T. Mandal and S. Seok, Nano Lett. 13, 1764 (2013).

[21] G. Eperon, S. Stranks, C. Menelaou, M. Johnston, L. Herz and H. Snaith, Energy Environ. Sci. 7, 982 (2014).

[22] T. Koh, K. Fu, Y. Fang, S. Chen, T. Sum, N. Mathews, S. Mhaisalkar, P. Boix and T. Baikie, J. Phys. Chem. C 118, 16458 (2014).

[23] T. Leijtens, G. Eperon, S. Pathak, A. Abate, M. Lee and H. Snaith, Nat. Commun. 4, 2885 (2013).

[24] H. Cho, S. Jeong, M. Park, Y. Kim, C. Wolf, C. Lee, J. Heo, A. Sadhanala, N. Myoung, S. Yoo, S. Im, R. Friend and T. Lee, Science 350, 1222 (2015).

[25] K. Lim, S. Ahn, Y. Kim, Y. Qi, T. Lee, Energy Environ. Sci. 9, 932 (2016).

[26] H. Kim, K. Lim, T. Lee, Energy Environ. Sci. 9, 12 (2016).

[27] K. Ali, S. Khan and M. Jafri, Sol. Energy 101, 1 (2014).

[28] L. Yao and J. He, Prog. Mater. Sci. 61, 94 (2014).

[29] P. Šiffalovič, M. Jergel, M. Benkovičová, A. Vojtko, V. Nádaždy, J. Ivančo, M. Bodík, M. Demydenko and E. Majková, Sol. Energy Mater. Sol. Cells 125, 127 (2014).

[30] G. Griffini, F. Bella, F. Nisic, C. Dragonetti, D. Roberto, M. Levi, R. Bongiovanni and S. Turri, Adv. Energy Mater. 5, 1401312 (2015).

[31] N. Chander, A. Khan, P. Chandrasekhar, E. Thouti, S. Swami, V. Dutta and V. Komarala, Appl. Phys. Lett. 105, 033904 (2014).

[32] M. Peng, X. Yin, P. Tanner, M. Brik and P. Li, Chem. Mater. 27, 2938 (2015).

[33] M. Peng, X. Yin, P. Tanner, C. Liang, P. Li, Q. Zhang, J. Qiu and A. Srivastava, J. Am. Chem. Soc. 96, 2870 (2013).

[34] P. Ndione, W. Yin, K. Zhu, S. Wei and J. Berry, J. Mater. Chem. A 3, 21940 (2015).

[35] A. Leguy, Y. Hu, M. Campoy-Quiles, M. Alonso, O. Weber, P. Azarhoosh, M. Schilfgaarde, M. Weller, T. Bein, J. Nelson, P. Docampo and P. Barnes, Chem. Mater. 27, 3397 (2015).

[36] J. Bai, X. Xu, L. Xu, J. Cui, D. Huang, W. Chen, Y. Cheng, Y. Shen, M. Wang, ChemSusChem 6, 622 (2013).

[37] Q. Bao, X. Liu, S. Braun and M. Fahlman, Adv. Energy Mater. 4, 201301272 (2014).

[38] J. You, L. Meng, T. Song, T. Guo, Y. Yang, W. Chang, Z. Hong, H. Chen, H. Zhou, Q. Chen, Y. Liu, N. De Marco and Y. Yang, Nat. Nanotech. 11, 75 (2016).

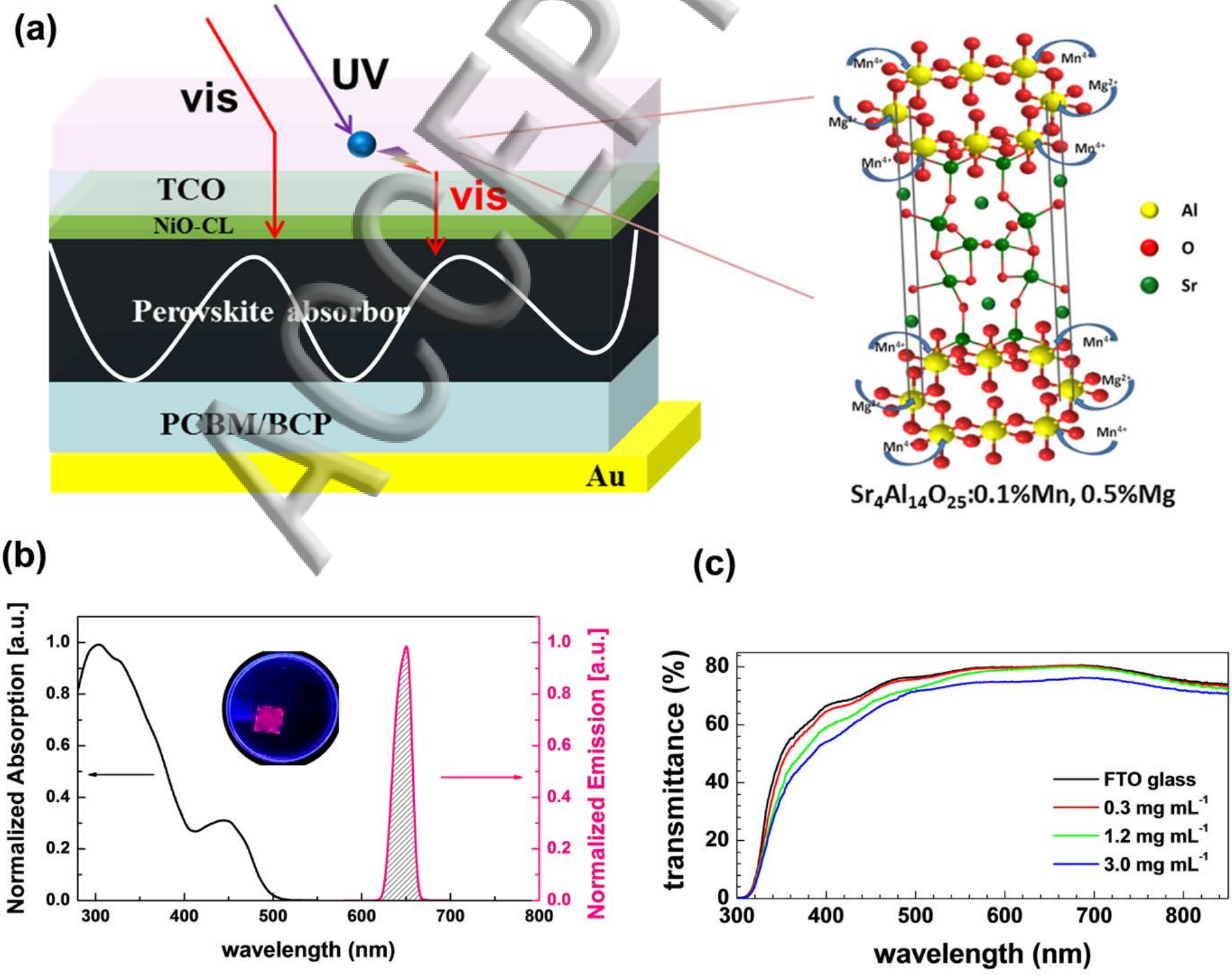
(a)
vis
UV
TCO
NiO-CL
vis
Perovskite absorber
PCBM/BCP
Au
Al
O
Sr
$Sr_4Al_{14}O_{25}$:0.1%Mn, 0.5%Mg
(b)
Normalized Absorption [a.u.]
Normalized Emission [a.u.]
wavelength (nm)
(c)
transmittance (%)
FTO glass
0.3 mg mL^{-1}
1.2 mg mL^{-1}
3.0 mg mL^{-1}
wavelength (nm)

(a)

Samples / conditions	Sample A covered $MAPbI_3$ / FTO	Sample B $MAPbI_3$ / FTO	Sample C SAM/PMMA coating / FTO / $MAPbI_3$
Ambient air	dark	UV	UV
Ambient air	dark	Yellow	Yellow
Dry air	dark	UV	UV

(b)

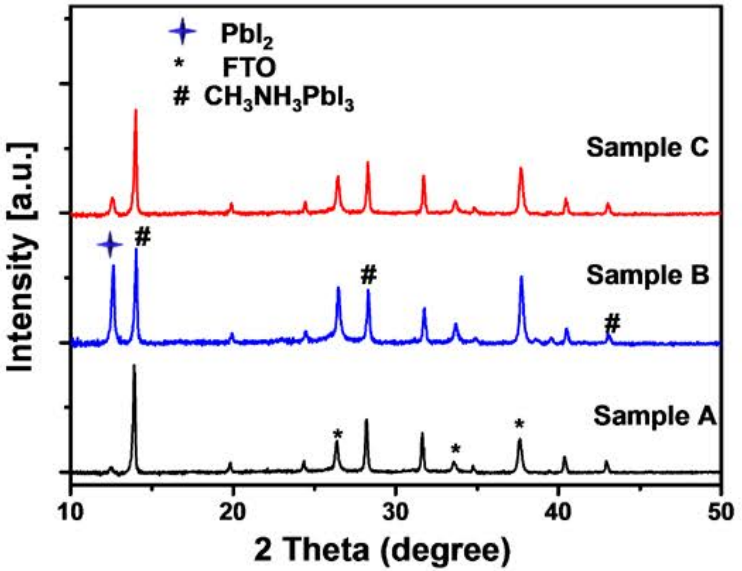

(c)

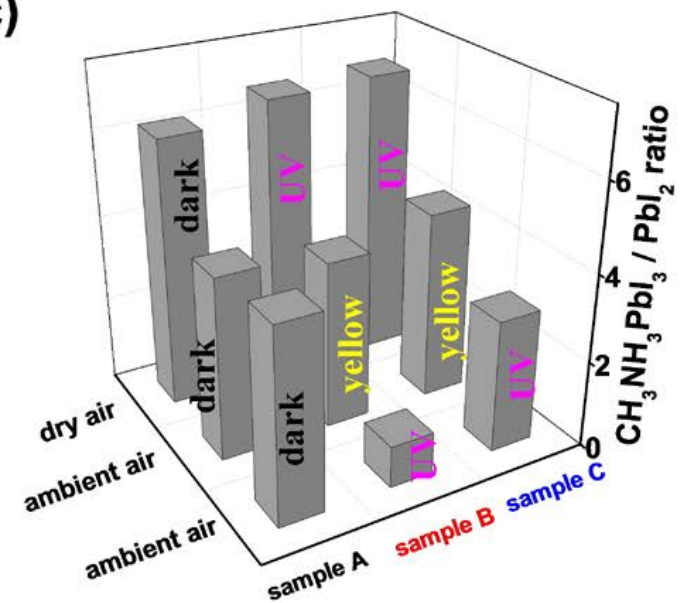

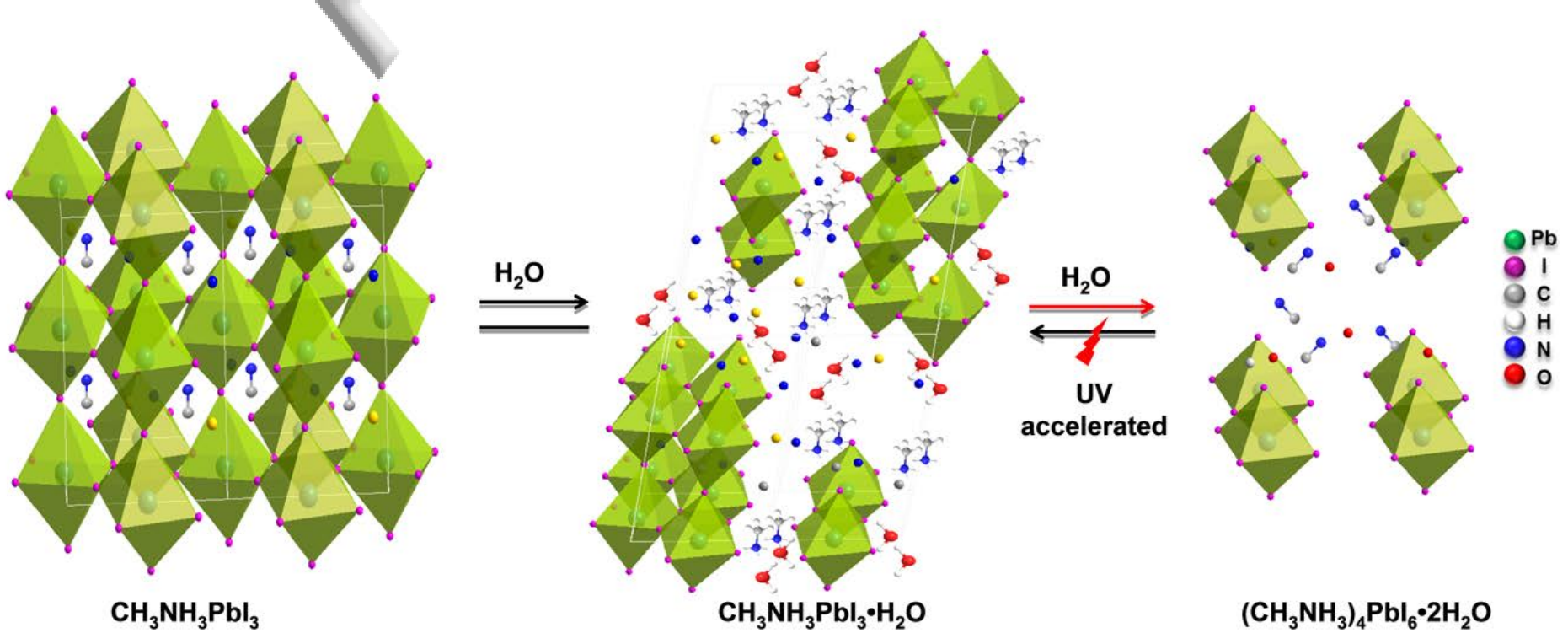
H2O
H2O
UV
accelerated
Pb
I
C
H
N
O
CH3NH3PbI3
CH3NH3PbI3•H2O
(CH3NH3)4PbI6•2H2O

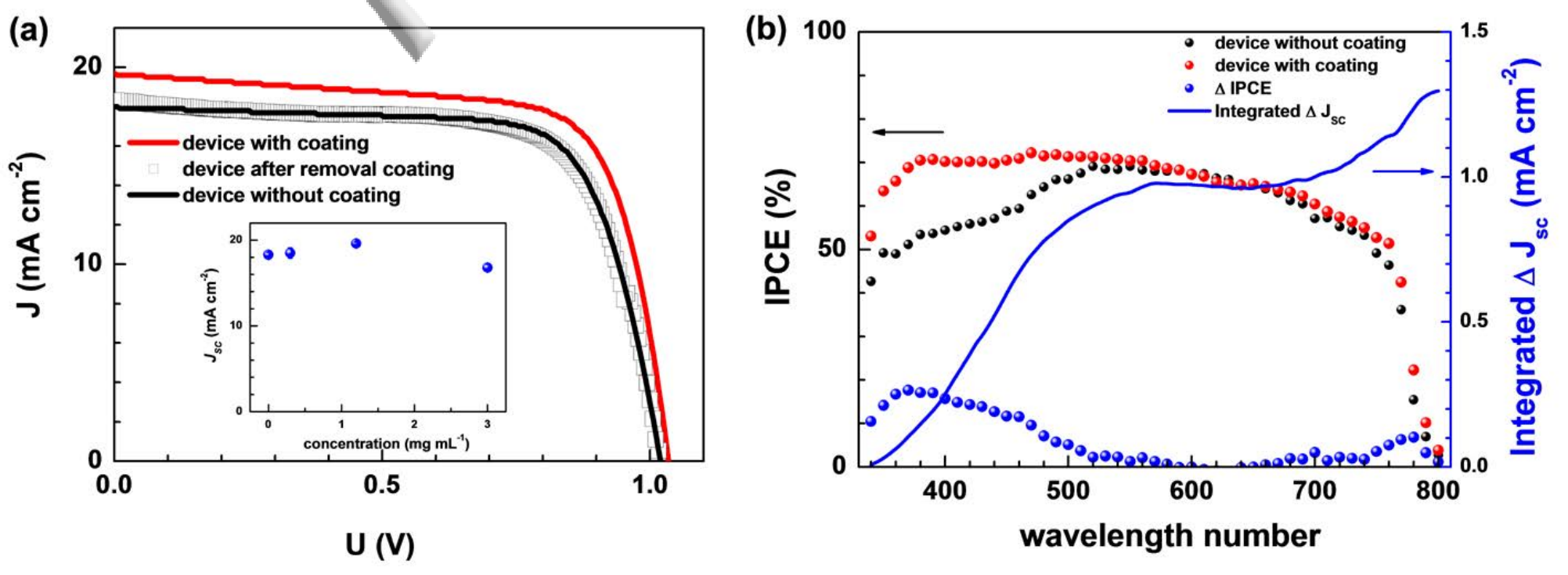
(a)
J (mA cm-2)
U (V)
device with coating
device after removal coating
device without coating
Jsc (mA cm-2)
concentration (mg mL-1)
(b)
IPCE (%)
wavelength number
device without coating
device with coating
Δ IPCE
Integrated Δ Jsc
Integrated Δ Jsc (mA cm-2)

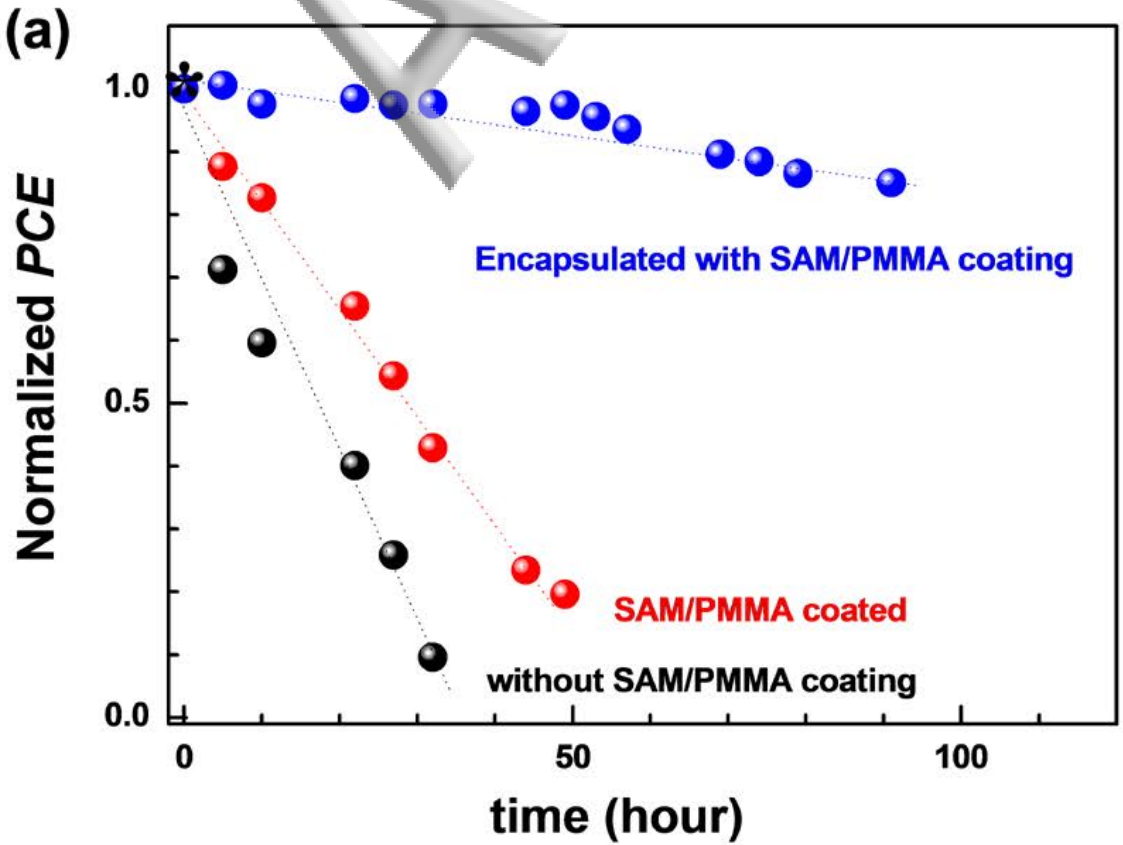
(a)
Normalized PCE
1.0
0.5
0.0
0
50
100
time (hour)
Encapsulated with SAM/PMMA coating
SAM/PMMA coated
without SAM/PMMA coating

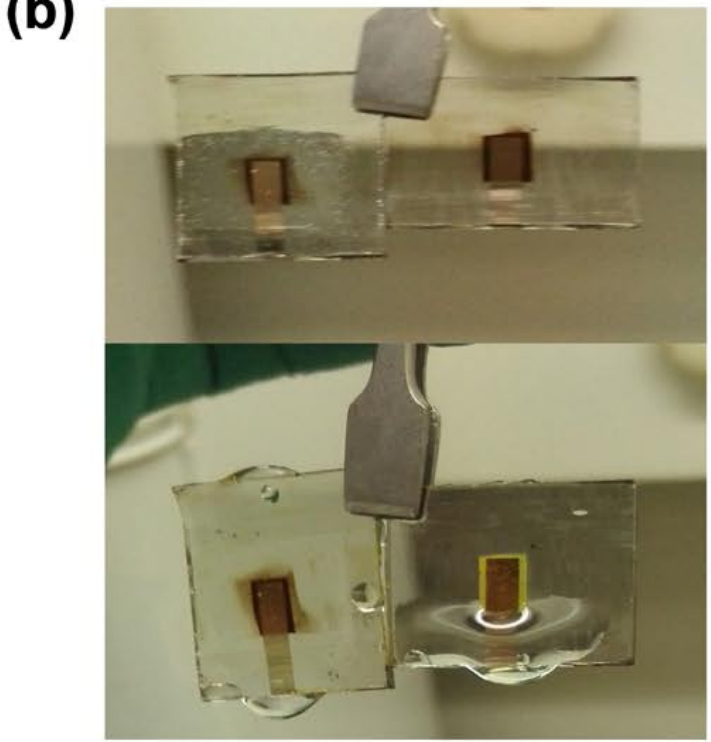
(b)